Journal of Radiological Protection

Official journal of the Society for Radiological Protection

ACCEPTED MANUSCRIPT

Decommissioning procedure and induced activation levels, calculations and measurements in an 18 MeV Medical Cyclotron

To cite this article before publication: Riccardo Calandrino *et al* 2021 *J. Radiol. Prot.* in press https://doi.org/10.1088/1361-6498/ac28f0

Decommissioning procedure and induced activation levels, calculations and measurements in an 18 MeV Medical Cyclotron

Riccardo Calandrino[1,*], Simone Manenti[2,3,*], Flavia Groppi[2,3], Francesco Broggi[3], Carlo Bergamaschi[4], Andrea Ferrari[4], Simona Manenti[4], Massimiliano Nizzi[4], Alessandro Loria[1], Antonella del Vecchio[1]

[1] Medical Physics Department, Ospedale San Raffaele Via Olgettina 60, I-20132 Milano, Italy

[2] Department of Physics, University of Milan, Via Celoria 16, I-20133 Milano, Italy

[3] Laboratorio Acceleratori e Superconduttività Applicata (LASA), Department of Physics, University Degli Studi di Milano and INFN-Milano, Via F.lli Cervi 201, I-20090 Segrate (MI), Italy

[4] Laboratorio Di Analisi Radiometriche Campoverde, Campoverde srl, Via Marco Fabio Quintiliano, 31, I-20138 Milano, Italy

[*] ***Riccardo Calandrino*** *and* ***Simone Manenti*** *contributed equally to this work and considered co-first authors*

Corresponding author: Riccardo Calandrino, Via Olgettina 60, I-20132 Milano, ITALY; phone +39 335 6709 626*; e mail:* calandrino.riccardo@hsr.it

Abstract

The present article describes the decommissioning of a self-shielded 18 MeV medical cyclotron IBA Cyclone 18/9 after 14 years of operation. A Monte Carlo simulation of the possible nuclear reactions was performed in order to plan the decommissioning activities. During the cyclotron dismantling, the activities of the cyclotron components, concrete wall and floor samples were

measured. Residual activities were analyzed by means of an HPGe detector and Liquid Scintillation Counting, and compared with simulation data. Dosimetry of the staff involved in the decommissioning procedure was monitored by individual TL dosimeters and/or digital dosimeter. The cyclotron component analysis confirmed the presence of gamma and pure beta emitters, ^{22}Na, ^{54}Mn, ^{60}Co, ^{65}Zn, ^{207}Bi, ^{55}Fe, ^{63}Ni at different values of specific activity, depending on the positioning of the sample point and on the alloy of the sampled part. In these components the presence of gamma and pure beta emitters was measured five years after the shutdown at levels far above clearance limits as defined by the "Recommended radiological protection criteria for the recycling of metals from the dismantling of nuclear installations" (RP89) guidelines. The simulation, carried out by FLUKA Code (version 2020.0.5) on the cyclotron components, provided good agreement with measurements, with a maximum discrepancy of the same order as the uncertainties.

Four engineers of the cyclotron maintenance staff were involved in the dismounting of the hottest components and rigging of the cyclotron in the deposit six months after shutdown and two engineers were involved during the drilling phase 3.5 years after shutdown. The measured dose from external exposure of the involved staff was lower than 100 μSv person^{-1} during the first phase and lower than 20 μSv person^{-1} during the final drilling phase. Measured doses from intake were negligible. In conclusion, the decommissioning of the 18 MeV cyclotron does not represent a risk for the involved staff, but, due to the presence of long-lived radioisotopes, the cyclotron components are to be treated as Low Level Radioactive Waste, and stored in an authorized storage area for at least 25 years after shutdown.

Key words: cyclotron; dosimetry; exposure, occupational; waste management

1. INTRODUCTION

In June 2015, the 18 MeV IBA Cyclotron was shut down after more than 14 years of continuous operation, having started in March 2001, in isotope production at the Nuclear Medicine Department of Istituto di Ricovero e Cura a Carattere Scientifico (IRCCS) Ospedale San Raffaele – Milano. The above-mentioned cyclotron was a self-shielded, negative ion accelerator, accelerating H^- ions up to 18 MeV and D^- ions up to 9 MeV; however the deuteron beam was never used. The maximum allowable proton current was 80 μA, while the average beam current on target was 40 μA. The cyclotron was used mainly to produce ^{18}F and ^{11}C by 18 MeV proton beams: the former by $^{18}O(p,n)^{18}F$ reaction, using a target of commercially available ^{18}O enriched water ($^{18}O > 94\%$), and the latter by $^{14}N(p,\alpha)^{11}C$, using a gaseous target mixture of $^{14}N + 1\%O_2$. The production of ^{13}N (ammonia labeled with nitrogen) by means of $^{16}O(p,\alpha)^{13}N$ by 18 MeV protons was added in the recent past. The workload of the cyclotron over the course of its operational life increased from an initial value of 170 μA·h·week^{-1} to 1 000 μA·h·week^{-1} in the period between 2006 and 2008, returning to a basic value of 400 μA·h·week^{-1} in the last years of its functioning. Fig. 1 shows the cyclotron workload up to the end of operations.

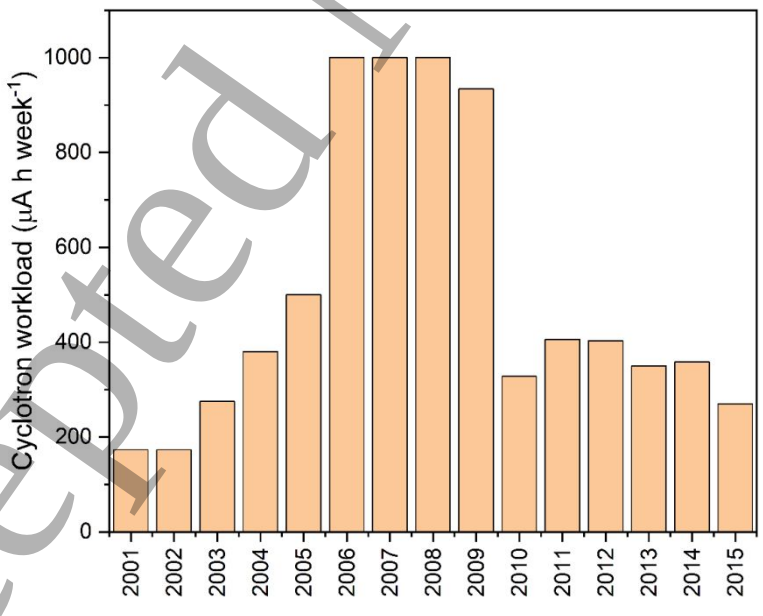

Figure 1. Workload of the cyclotron from 2001 to 2015.

The increased high load clinical activity of the PET cyclotron in the Nuclear Medicine Department (approximately 40 patients per day in 2015) demanded an efficient and reliable radioisotope production system, and led to the replacement of the existing 18 MeV IBA Cyclone with a new unit more suitable for the new requirements, and perfectly matching the on-site shielding system. In any case, it was necessary to address and resolve several problems related to the decommissioning of the old cyclotron, including the partial demolition and reconstruction of the lateral wall of the cyclotron room, where an exit and entrance aperture was created in order to move out the old cyclotron and to move in the new one.

Several published papers report data on the activation of beam transport components [1-5], of the cyclotron vault [6-10] or linear accelerator [11-14]. No data have been found for 18 – 20 MeV energy self-shielded cyclotron accelerators, despite the fact that this type of cyclotron is currently one of the most suitable and widely used instruments for isotope production.

This article presents all the data and calculations collected concerning the activation level of the main cyclotron components, as well as data and estimates relative to equivalent body doses for staff involved in the dismantling and rigging of the removed cyclotron.

2. MATERIALS AND METHODS

Table 1. Predicted reactions yielding radioactive isotopes with half-life greater than 27 days.

Nuclide	Reaction	Activated element	Half-Life
^{65}Cu	(p,n)	^{65}Zn	244.06 (d)
^{109}Ag	(p,n)	^{109}Cd	461.00 (d)
^{181}Ta	(p,n)	^{181}W	121.20 (d)
^{22}Na	(n,α2n)	^{27}Al	2.60 (y)
^{58}Ni	(n,p)	^{58}Co	70.81 (d)
^{58}Ni	(n,α)	^{55}Fe	2.70 (y)
^{60}Ni	(n,p)	^{60}Co	5.27 (y)
^{62}Ni	(n,γ)	^{63}Ni	100.10 (y)
^{62}Ni	(n,α)	^{59}Fe	44.64 (d)
^{54}Fe	(n,γ)	^{55}Fe	2.70 (y)
^{58}Fe	(n,γ)	^{59}Fe	44.64 (d)
^{59}Co	(n,γ)	^{60}Co	5.27 (y)

The induction of radioactivity into the cyclotron components (Table1) [15] are originated by means of:

- direct interaction of the accelerated ion with the beam transport devices (vacuum chamber), RF system (Dees and central region and RF cavity sheets), stripping foil holder, foils, target (for the first group of elements in Table 1);
- interaction of the proton reaction generated neutrons with all the materials outside the vacuum chamber, such as the magnet coils and the yoke structure (for the second group of elements in Table 1).

The expected activation levels of various components, as reported in the literature for high energy machines, are summarized in Table 2 [16].

Table 2. Expected activation levels for different cyclotron and shielding components.

Item	Weight (kg)	Expected activity class ($Bq \cdot g^{-1}$)
Magnet system[a]	20 400	0.4 - 200
Magnet coils	2 400	0.4 -200
Vacuum Chamber	200	1.0 - 200
RF System	35	0.1 – 0.4
Targets	10	1.0 - 200
Ion Source	5	1.0 - 200
Shields	16 000	0.4 - 200
Perimetric walls		0.1 – 0.4
Cyclotron Vault floor		0.1 – 0.4

[a] Main and return yokes and poles

In our case, the cyclotron shielding will remain in place and in use for the new cyclotron, thus, this work is focused on the study and measurement of the activation induced in the cyclotron.
Among the components of the cyclotron, the magnet (*i.e.,* magnet system and coils) represent 99% (in weight) of the activated parts. A suitable storage site, specifically equipped for the final storage of large, dismantled parts, and corresponding to Italian national authorization procedure for radioactive waste storage, was located on the Hospital estate, far removed from the clinical area.

2.1 FLUKA Simulation

Before the beginning of the sampling of the cyclotron, a thorough monitoring of various operational points around the two halves of the unit was carried out by the Health Physics personell with a plastic scintillator (AUTOMESS 6150 ADB, ZnS-coated) to evaluate the risk for involved staff. FLUKA version 2020.0.5 [17,18] and the user interface Flair version 2.3-0 [19] were subsequently adopted in order to predict the activation of the cyclotron's components: magnet (upper and lower yoke), return yoke, and coils (Fig. 2).

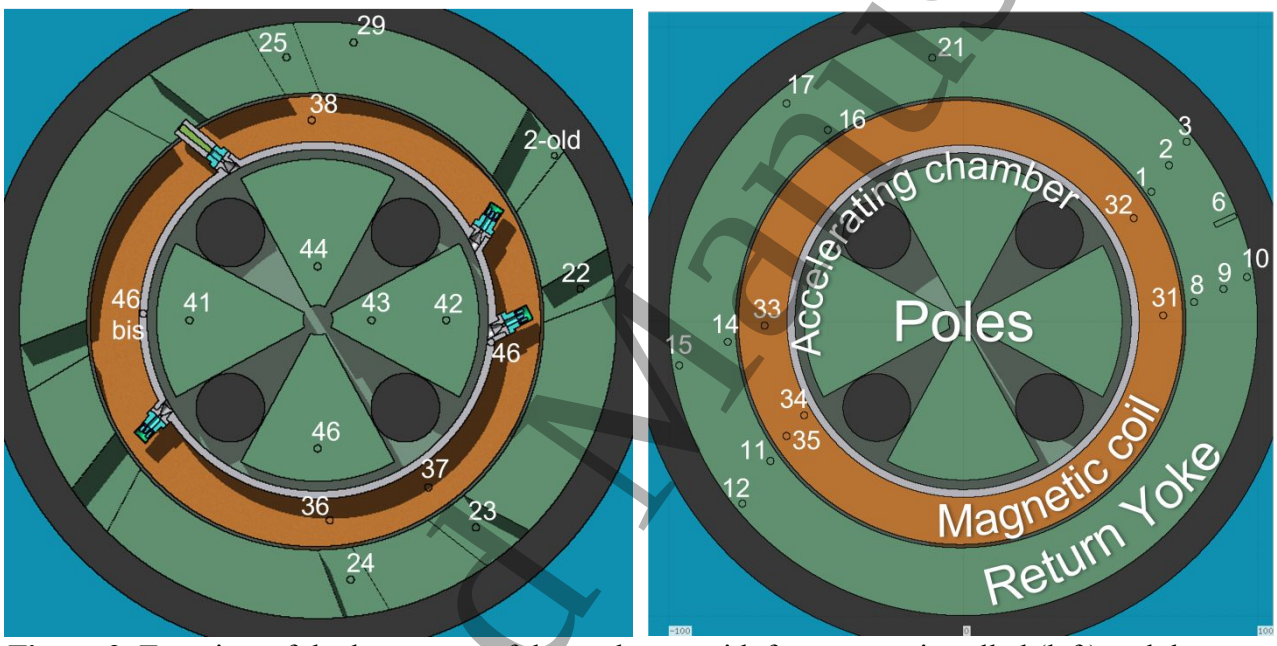

Figure 2. Top view of the lower part of the cyclotron with four targets installed (left) and the upper one with some analysed samples (circle with ID numbers).

The simulation was conducted on the basis of the detailed workload of the cyclotron, and on the composition datasheet of the main cyclotron components.

The vacuum chamber integrated the targets for the production of radionuclides, meaning that beam protons did not contribute directly to the radioactivation of some of the main components of the cyclotron outside the vacuum chamber (*i.e.,* coils and yokes). The interaction of the proton beam particles on the targets induced secondary neutrons (*e.g.,* Fig. 3, spectrum of the neutrons produced by the reaction $H_2{}^{18}O(p,y+xn)$).

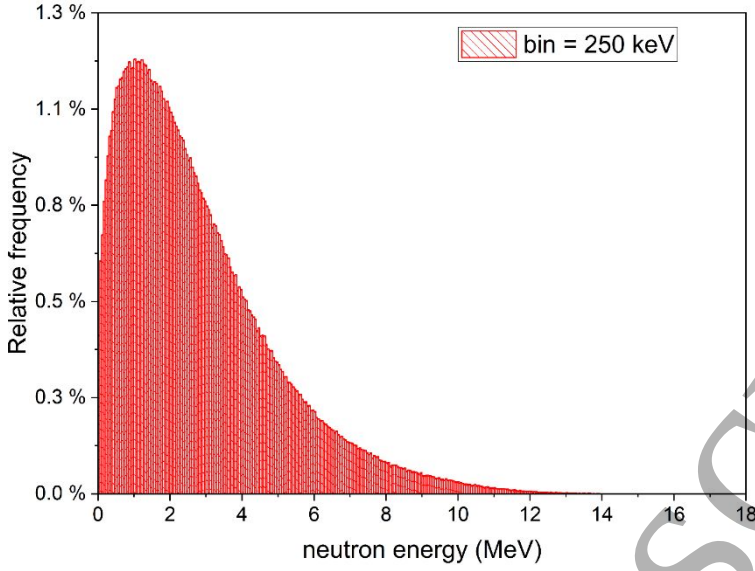

Figure 3. Neutron energy spectrum per primary proton generated by the reaction $H_2{}^{18}O(p,y+xn)$. This neutron distribution was produced by FLUKA 2020.0.5.

Radioactivation was simulated on 53 sampling points (see Section 2.2) and on the following macro sub-systems: magnet coils, main and return yokes, poles and vacuum chamber.

2.2 Sampling and measurements

To evaluate the activation of the cyclotron components, magnet (upper and lower yoke), return yoke, poles, dees and all the largest components, 53 samples were taken at different points from all the components of the cyclotron (Figures 2 and 4).

The cyclotron samples were obtained by drilling holes of 2.5 cm diameter and 10 cm depth into the different components. The points were chosen following geometrical criteria in order to appropriately represent extended components with a finite number of samples. The cyclotron is composed of two shells. These two halves were separated, using a crane, to facilitate the sampling on each inner side.

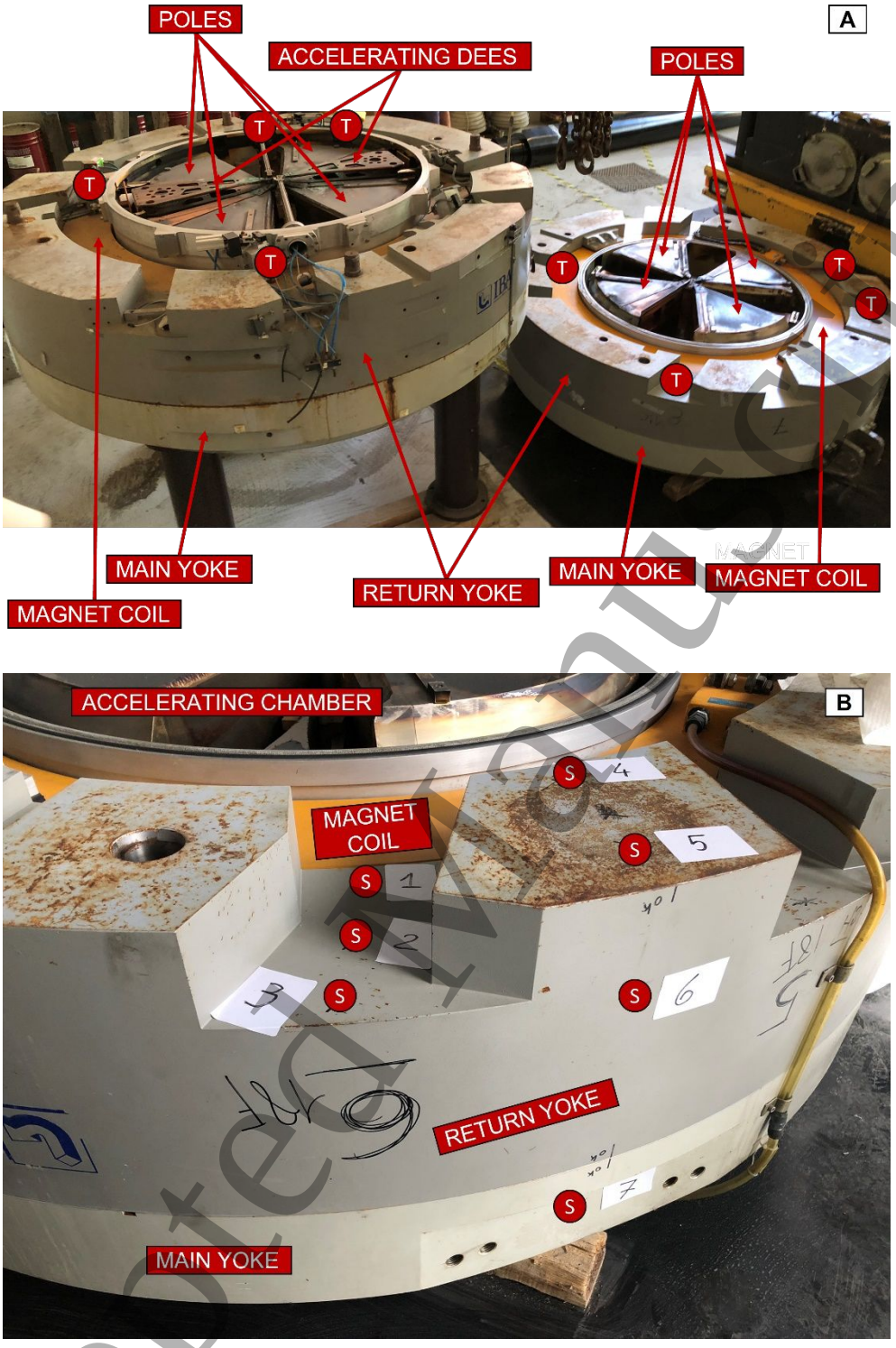

Figure 4. Separated halves of the cyclotron: (**A**) cyclotron main components and the positions of the used targets (T) and (**B**) example of seven sampling points (S) identified by the ID numbers 1-7.

For the gamma spectroscopy measurements, 70 – 80 g of sample was cleaned in an ultrasonic bath. All samples were dried at 70°C for 24 h until they reached a constant mass.

The samples were inserted in Petri dish containers after cleaning was completed (Figure 5).

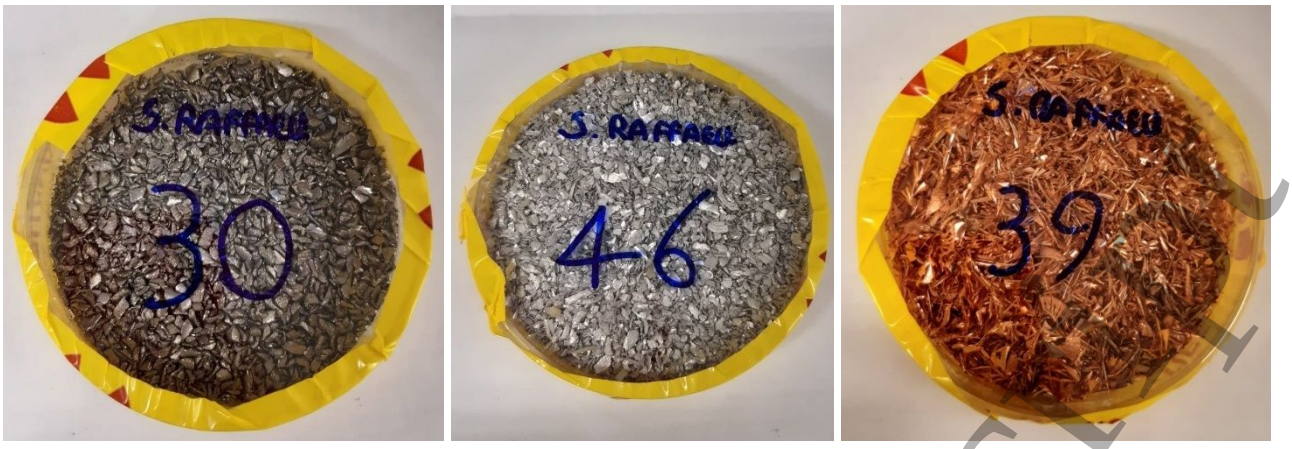

Figure 5. Material samples. See Table 4 for description and matrix composition.

In order to obtain a suitable sample for Liquid Scintillation Counting (LSC) analysis, 1.5-2 g of solid sample was dissolved in an HNO_3 plus HCl solution on a heating plate. A known quantity of the sample was then transferred to a beaker, together with a known quantity of stable Carrier ($Fe(NO_3)_3 \cdot 9H_2O$ and $Ni(NO_3)_2 \cdot 6H_2O$). The obtained sample was then centrifuged (2500 rpm, 20 min).

Chemical separation of ^{55}Fe was performed by means of TRU Resin (Triskem), while separation of ^{63}Ni was carried out through Ni-Resin (Triskem).

The gamma emission activation products present in each sample were determined by a high-resolution gamma spectroscopy system, using a coaxial n-type HPGe detector (Itech Instruments, model NIGC 3019) with relative efficiency of 30% and energy resolution of 1.9 keV, both referring to the 1.332 MeV ^{60}Co emission. The efficiency calibration was performed using WinnerTrack (Itech Instruments) on a characterized detector and verified using a liquid multi-gamma DAkkS certified solution by Eckert&Ziegler (S.N. 2155-45-1, Calibration mark: 2020-06). This source, produced in disk geometry, is suitable to cover a 46 keV – 1830 keV energy range. The spectrum was acquired using a 16k multichannel analyser (Orion Itech Instruments) and the post analysis of gamma-ray spectra was carried out by means of InterWinner 7.0 software. All measurements were performed in a 15 cm thick multi-layer shielding (Pb → Cu → Cd) to reduce the terrestrial and

extra-terrestrial natural radiation background. The minimum detectable activity (MDA) of the system was calculated according to Currie [20].

Beta and X-ray emitter induced activities (as ^{55}Fe and ^{63}Ni) were determined by the TR-LSC system Quantulus GCT-6220 (PerkinElmer) using active and passive systems to perform measurements in low level background mode. The efficiency calibration was carried out by counting both ^{55}Fe and ^{63}Ni quench curves, which allow the calculation of the efficiency value for each sample (according to the tSIE value). The quench curves were made using a DAkkS certified solution by Eckert&Ziegler (^{55}Fe: S.N.:1921-33, Calibration mark: 2017-04, ^{63}Ni: S.N. 77672/5, Calibration mark: 2012-08). The analysis window used is 0-6 keV for ^{55}Fe and 0-66 keV for ^{63}Ni.

Ultima Gold LLT was used as scintillation cocktail in an 8-to-12 sample-to-cocktail ratio.

In LSC measurements the minimum detectable activity (MDA) was calculated in accordance with ISO 11929-1:2019 [21], with k=1.645 uncertainty cover factor, corresponding to a 95% confidence level.

2.3 Environmental and staff radioprotection and safety

Concerning environmental and staff radioprotection and safety, the decommissioning procedures were scheduled as shown in Table 3 [22].

Table 3. Decommissioning and sampling program.

Phase #	Days after shutdown	Operations
0	Day 0 (15/06/2015)	Cyclotron shutdown
1	Day 36	Dismantling targets, vacuum pumps and cyclotron power supply by IBA staff
2	Day 169-178	Training course for demolition workers, wall demolition and cyclotron move out
3	Day 1644 (4.5 years)	Samples taken from the cyclotron components by means of drilling in selected points

This schedule calls for the preliminary dismantling of the easiest (in terms of the dismantling process) and hottest components (i.e., targets and vacuum Pumps) from the cyclotron after a brief waiting period after the last beam (Phase 1). The second step was the sealing of the cyclotron room in order to guarantee the insulation of nearby rooms and corridors from ducts. Before the start of demolition operations, a complete training program concerning the safety rules and procedures to be followed during the operation was carried out by the Radiation Protection Expert. In particular, as the demolition of the floor area located below the targets was considered the most dangerous phase, the main prescriptions regarding this operation were:

- operating personnel were instructed to wear gas masks (carbon filtered) and sealed suits to prevent radioactive dust inhalation;
- the use of a suitable drilling tool equipped with a vacuum pump and a dust collection tank was mandatory.

The Medical Physics Department staff supervised all phases of the decommissioning, and collected radiation exposure data for both environment and operating personnel:

- dose and dose-rate values in the operating room were measured using an organic scintillator probe (AUTOMESS 6150 ADB, ZnS-coated) for the real time measurement of the local background (minimum sensitivity 50 nSv · h^{-1} s.d. <15%);
- 8 LiF (Mg, Cu, P) TLD dosimeters, type GR 200 A, without filtration (minimum sensitivity 4 μGy at 1.25 MeV) were positioned on the walls for the duration of the entire procedure, for the measurement of the environmental dose;
- LiF TLD, card with three dosimeters, two filtered (1 mm Al and 1 mm Cu) and one unfiltered, were used as personal body dosimeters;
- daily surface contamination tests on various employed tools (*e.g.,* hammers, drills) as well as external (clothing) and internal (urine samples, spit and nasal mucus) tests for personnel were performed as described in Calandrino et al, 2009 [23], and measured by means of NaI

gamma counter (LKB Wallac energy resolution = 8.4 keV and efficiency= 9% at 661.7 keV of ^{137}Cs).

In the third and last phase, samples were taken from the cyclotron components by means of drilling in selected points as described above.

3. RESULTS AND DISCUSSION

The results of main gamma-emission nuclide vectors found in samples collected at different points for the cyclotron components are presented in Table 4. Results are presented in comparison with the FLUKA simulation.

Table 4. Activity concentrations of the ^{22}Na, ^{54}Mn, ^{57}Co, ^{60}Co, ^{65}Zn and ^{207}Bi in the samples.

			Activity Concentrations [Bq g^{-1}]							
ID	**Description**	**Matrix**	**^{22}Na**	**^{54}Mn**		**^{57}Co**	**^{60}Co**		**^{65}Zn**	**^{207}Bi**
			EXP.	**EXP.**	**FLUKA**	**EXP.**	**EXP.**	**FLUKA**	**EXP.**	**EXP.**
\\	Upper return yoke, OUT 6, 2 cm from inner border	Magnetic steel IBA	< 0.002	3.8 ± 0.4	6.9 ± 0.2	< 0.01	5.4 ± 0.6	3.7 ± 0.6	< 0.006	< 0.0015
2	Upper return yoke, OUT 6, 12 cm from inner border	Magnetic steel IBA	< 0.002	5.1 ± 0.5	1.88 ± 0.08	< 0.01	7.2 ± 0.7	3.2 ± 0.3	< 0.006	< 0.0015
3	Upper return yoke, OUT 6, 18 cm from inner border	Magnetic steel IBA	< 0.002	1.55 ± 0.09	0.98 ± 0.05	< 0.01	2.32 ± 0.13	3.4 ± 0.5	< 0.006	< 0.0015
4	Upper return yoke, OUT 5-6, 2 cm from inner border	Magnetic steel IBA	< 0.002	3.6 ± 0.2	9.5 ± 0.3	< 0.01	7.9 ± 0.4	3.7 ± 0.5	< 0.006	< 0.0015
5	Upper return yoke, OUT 5-6, 14 cm from inner border	Magnetic steel IBA	< 0.002	0.52 ± 0.03	0.47 ± 0.05	< 0.01	2.80 ± 0.16	3.2 ± 0.4	< 0.006	< 0.0015
6	Upper return yoke, OUT 5-6, outer side	Magnetic steel IBA	< 0.002	0.41 ± 0.03	0.28 ± 0.05	< 0.01	2.81 ± 0.16	3.2 ± 0.5	< 0.006	< 0.0015
7	Upper main yoke, OUT 5-6, outer side	Magnetic steel IBA	< 0.002	0.20 ± 0.01	0.013 ± 0.010	< 0.01	1.31 ± 0.07	1.3 ± 0.5	< 0.006	< 0.0015
8	Upper return yoke, OUT 5, 2 cm from inner border	Magnetic steel IBA	< 0.002	17.2 ± 1.8	21.2 ± 0.5	< 0.01	10.1 ± 1.0	7.0 ± 0.4	< 0.006	< 0.0015
9	Upper return yoke OUT 5, 12 cm from inner border	Magnetic steel IBA	< 0.002	8.5 ± 0.5	7.2 ± 0.4	< 0.01	5.2 ± 0.3	5.3 ± 0.7	< 0.006	< 0.0015
10	Upper return yoke, OUT 5, 18 cm from inner border	Magnetic steel IBA	< 0.002	6.6 ± 0.4	3.4 ± 0.3	< 0.01	4.5 ± 0.3	5.5 ± 0.9	< 0.006	< 0.0015
11	Upper return yoke, OUT 2, 2 cm from inner border	Magnetic steel IBA	< 0.002	20.3 ± 1.2	10.7 ± 4.5	< 0.01	8.2 ± 0.5	2.4 ± 0.3	< 0.006	< 0.0015

ID	Description	Matrix	Activity Concentrations [Bq g^{-1}]							
			^{22}Na	^{54}Mn		^{57}Co	^{60}Co		^{65}Zn	^{207}Bi
			EXP.	EXP.	FLUKA	EXP.	EXP.	FLUKA	EXP.	EXP.
12	Upper return yoke, OUT 2, 18 cm from inner border	Magnetic steel IBA	< 0.002	6.0 ± 0.6	2.4 ± 0.2	< 0.01	3.1 ± 0.3	0.7 ± 0.4	< 0.006	< 0.0015
13	Upper return yoke, OUT 2-1, 10 cm from inner border	Magnetic steel IBA	< 0.002	0.67 ± 0.07	2.2 ± 0.1	< 0.01	2.5 ± 0.3	1.43 ± 0.17	< 0.006	< 0.0015
14	Upper return yoke, OUT 1, 2 cm from inner border	Magnetic steel IBA	< 0.002	0.58 ± 0.06	0.98 ± 0.10	< 0.01	3.2 ± 0.3	1.3 ± 0.2	< 0.006	< 0.0015
15	Upper return yoke, OUT 1, 18 cm from inner border	Magnetic steel IBA	< 0.002	0.158 ± 0.010	0.055 ± 0.018	< 0.01	1.73 ± 0.10	1.1 ± 0.3	< 0.006	< 0.0015
16	Upper return yoke, OUT 8, 2 cm from inner border	Magnetic steel IBA	< 0.002	7.9 ± 0.5	12.2 ± 0.5	< 0.01	2.52 ± 0.14	1.2 ± 0.2	< 0.006	< 0.0015
17	Upper return yoke, OUT 8, 18 cm from inner border	Magnetic steel IBA	< 0.002	2.7 ± 0.2	2.8 ± 0.2	< 0.01	1.06 ± 0.06	0.8 ± 0.2	< 0.006	< 0.0015
18	Upper return yoke, OUT 8-7, 18 cm from inner border	Magnetic steel IBA	< 0.002	2.1 ± 0.2	0.64 ± 0.11	< 0.01	0.91 ± 0.09	1.0 ± 0.2	< 0.006	< 0.0015
19	Upper return yoke, OUT 8, outer side	Magnetic steel IBA	< 0.002	0.73 ± 0.05	0.19 ± 0.09	< 0.01	0.75 ± 0.04	1.4 ± 0.5	< 0.006	< 0.0015
20	Upper main yoke, OUT 8, outer side	Magnetic steel IBA	< 0.002	0.035 ± 0.003	NA	< 0.01	0.37 ± 0.02	0.14 ± 0.07	0.007 ± 0.003	0.030 ± 0.002
21	Upper return yoke, OUT 7, 14 cm from inner border	Magnetic steel IBA	< 0.002	0.091 ± 0.010	0.22 ± 0.07	< 0.01	0.83 ± 0.09	0.48 ± 0.16	0.014 ± 0.005	< 0.0015
22	Lower return yoke, OUT 5, 14 cm from inner border	Magnetic steel IBA	0.009 ± 0.003	13.1 ± 0.8	6.9 ± 0.4	< 0.01	8.4 ± 0.5	4.4 ± 0.4	< 0.006	0.208 ± 0.013
23	Lower return yoke, OUT 4, 14 cm from inner border	Magnetic steel IBA	0.0021 ± 0.0008	0.044 ± 0.004	0.04 ± 0.02	< 0.01	0.79 ± 0.05	1.9 ± 0.5	0.014 ± 0.004	< 0.0015

ID	Description	Matrix	Activity Concentrations [Bq g^{-1}]							
			^{22}Na	^{54}Mn		^{57}Co	^{60}Co		^{65}Zn	^{207}Bi
			EXP.	EXP.	FLUKA	EXP.	EXP.	FLUKA	EXP.	EXP.
24	Lower return yoke, OUT 3, 14 cm from inner border	Magnetic steel IBA	< 0.002	0.064 ± 0.005	0.04 ± 0.03	< 0.01	0.67 ± 0.04	0.9 ± 0.3	0.016 ± 0.004	< 0.0015
25	Lower return yoke, OUT 7, 14 cm from inner border	Magnetic steel IBA	0.020 ± 0.002	0.147 ± 0.010	0.14 ± 0.05	< 0.01	1.05 ± 0.06	1.0 ± 0.2	0.073 ± 0.007	< 0.0015
26	Lower return yoke, OUT 7, outer side	Magnetic steel IBA	0.0066 ± 0.0012	0.059 ± 0.010	NA	< 0.01	0.43 ± 0.04	0.45 ± 0.14	0.028 ± 0.004	0.0055 ± 0.0011
27	Lower main yoke, OUT 7, outer side	Magnetic steel IBA	0.0027 ± 0.0006	0.010 ± 0.002	NA	< 0.01	0.26 ± 0.02	0.30 ± 0.12	0.013 ± 0.003	< 0.0015
28	Lower main yoke, OUT 5, outer side	Magnetic steel IBA	0.003 ± 0.001	0.044 ± 0.005	0.06 ± 0.03	< 0.01	1.32 ± 0.13	1.8 ± 0.4	< 0.006	< 0.0015
29	Lower return yoke, OUT 6-7, outer side	Magnetic steel IBA	< 0.002	0.052 ± 0.004	0.07 ± 0.04	< 0.01	0.73 ± 0.04	0.8 ± 0.2	< 0.006	< 0.0015
30	Lower return yoke, OUT 6-7, outer side	Magnetic steel IBA	< 0.002	0.011 ± 0.002	0.04 ± 0.03	< 0.01	0.65 ± 0.07	0.9 ± 0.2	< 0.006	< 0.0015
1-OLD	Lower return yoke, OUT 6	Magnetic steel IBA	< 0.002	1.31 ± 0.09	NA	< 0.01	2.53 ± 0.15	NA	< 0.006	< 0.0015
2-OLD	Lower return yoke, OUT 6, outer side	Magnetic steel IBA	< 0.002	2.6 ± 0.3	NA	< 0.01	2.7 ± 0.3	NA	< 0.006	< 0.0015
31	Upper magnetic coil, OUT 5, center	OFCu[a]	< 0.002	6.0 ± 0.4	NA	< 0.01	4.1 ± 0.2	5904 ± 4.3	< 0.006	< 0.0015
32	Upper magnetic coil, OUT 6, center	OFCu	< 0.002	0.036 ± 0.006	NA	< 0.01	10.1 ± 0.6	16.1 ± 1.0	< 0.006	< 0.0015
33	Upper magnetic coil, OUT 1, center	OFCu	< 0.002	< 0.005	NA	< 0.01	3.1 ± 0.2	0.47 ± 0.15	< 0.006	< 0.0015
34	Upper magnetic coil, OUT 2, internal part	OFCu	0.014 ± 0.004	< 0.005	NA	< 0.01	20.8 ± 1.2	11.0 ± 1.1	< 0.006	< 0.0015
35	Upper magnetic coil, OUT 2, external part	OFCu	< 0.002	< 0.005	NA	< 0.01	4801 ± 5.5	24.8 ± 1.1	< 0.006	< 0.0015
36	Lower magnetic coil, OUT 3, center	OFCu	< 0.002	0.015 ± 0.002	NA	< 0.01	0.64 ± 0.04	NA	< 0.006	0.0017 ± 0.0005
37	Lower magnetic coil, OUT 5, center	OFCu	0.0030 ± 0.0007	< 0.005	NA	< 0.01	0.63 ± 0.07	NA	< 0.006	< 0.0015

ID	Description	Matrix	Activity Concentrations [Bq g^{-1}]							
			^{22}Na	^{54}Mn		^{57}Co	^{60}Co		^{65}Zn	^{207}Bi
			EXP.	EXP.	FLUKA	EXP.	EXP.	FLUKA	EXP.	EXP.
38	Lower magnetic coil, OUT 7, center	OFCu	0.037 ± 0.004	< 0.005	NA	< 0.01	1.04 ± 0.11	1.0 ± 0.4	0.029 ± 0.005	< 1.5 × 10^{-3}
39	Dee; internal part	Cu	< 0.002	< 0.005	NA	< 0.01	0.87 ± 0.0549	NA	0.095 ± 0.008	0.039 ± 0.003
40	Dee; external part	Cu	1.44 ± 0.08	0.47 ± 0.03	NA	0.023 ± 0.013	4.0 ± 0.2	NA	0.37 ± 0.03	0.037 ± 0.002
41	Lower pole, OUT 1, external part	Magnetic steel IBA	0.63 ± 0.04	3.4 ± 0.2	0.37 ± 0.08	0.86 ± 0.04	2.82 ± 0.16	1.4 ± 0.2	7.1 ± 0.4	0.008 ± 0.002.0
42	Lower pole, OUT 5, external part	Magnetic steel IBA	0.007 ± 0.002	0.86 ± 0.05	2.09 ± 0.13	0.096 ± 0.005	4.2 ± 0.2	5.2 ± 0.4	0.117 ± 0.011	< 0.0015
43	Lower pole, OUT 5, internal part	Magnetic steel IBA	0.030 ± 0.003	0.15 ± 0.01	0.12 ± 0.03	< 0.01	1.92 ± 0.11	2.1 ± 0.3	0.102 ± 0.009	0.0072 ± 0.0013
44	Lower pole, OUT 7, internal part	Magnetic steel IBA	0.022 ± 0.003	0.132 ± 0.014	0.20 ± 0.05	< 0.01	1.43 ± 0.15	1.8 ± 0.2	0.15 ± 0.02	< 0.0015
45	Lower pole, OUT 3, external part	Magnetic steel IBA	0.015 ± 0.002	0.37 ± 0.02	0.13 ± 0.03	< 0.01	1.84 ± 0.10	2.2 ± 0.3	0.36 ± 0.02	0.0056 ± 0.0012
46	Lower vacuum chamber, OUT 5	aluminium	2.4 ± 0.3	0.094 ± 0.011	NA	0.045 ± 0.005	0.23 ± 0.02	NA	0.21 ± 0.02	1.8 ± 0.2
46 bis	Lower vacuum chamber, OUT 1	aluminium	0.24 ± 0.03	0.011 ± 0.002	NA	0.015 ± 0.002	0.084 ± 0.009	NA	0.106 ± 0.012	0.042 ± 0.005
47	Upper pole, OUT 5, external part	Magnetic steel IBA	0.007 ± 0.002	0.67 ± 0.04	1.78 ± 0.15	< 0.01	3.6 ± 0.2	5.1 ± 0.5	0.035 ± 0.008	< 0.0015
48	Upper pole, OUT 5, external part	Magnetic steel IBA	0.0028 ± 0.0011	0.254 ± 0.016	0.07 ± 0.03	< 0.01	1.62 ± 0.09	2.3 ± 0.3	0.33 ± 0.02	< 0.0015
49	Upper pole, OUT 1, external part	Magnetic steel IBA	0.017 ± 0.002	1.6 ± 0.2	0.44 ± 0.08	0.19 ± 0.02	2.5 ± 0.3	1.6 ± 0.2	0.51 ± 0.06	< 0.0015
50	Upper pole, OUT 7, external part	Magnetic steel IBA	0.0047 ± 0.0011	0.56 ± 0.03	0.11 ± 0.04	0.156 ± 0.006	1.61 ± 0.09	2.2 ± 0.3	0.147 ± 0.011	< 0.0015

[a] Oxygen Free Copper

Results of the LSC measurements in the samples collected from the cyclotron components at various specific and representative points are presented in Tables 5 and 6.

Table 5. Activity concentrations of the ^{55}Fe in the samples. See Table 4 for description and matrix composition.

ID	^{55}Fe [Bq g^{-1}]	
	EXP.	FLUKA
2	50 ± 15	93.0 ± 2.4
3	86 ± 17	89.7 ± 3.3
5	160 ± 26	98.4 ± 2.3
6	41 ± 14	104 ± 3
7	70 ± 17	41.3 ± 1.7
9	170 ± 24	179 ± 3
10	154 ± 23	165 ± 7
12	80 ± 18	62.5 ± 1.6
13	97 ± 19	61.8 ± 1.7
15	41 ± 14	36.7 ± 1.6
17	78 ± 18	39.0 ± 3.2
18	61 ± 16	24.7 ± 1.9
19	82 ± 17	26.1 ± 1.8
20	< 29	15.4 ± 1.4
21	135 ± 21	24.7 ± 1.6
23	< 29	32.1 ± 1.5
24	< 29	24.7 ± 1.4
25	74 ± 14	28.5 ± 1.8
26	70 ± 17	21.2 ± 1.78
27	55 ± 16	12.7 ± 1.1
28	66 ± 15	51.8 ± 2.4
29	79 ± 16	24.5 ± 1.5
30	< 29	27.4 ± 1.9
41	126 ± 20	49.4 ± 1.6
42	188 ± 26	161 ± 2
43	58 ± 16	71.8 ± 2.2
44	301± 34	57.3 ± 2.1
46	52 ± 16	55.1 ± 2.0
47	192 ± 16	162 ± 3
48	< 29	23.8 ± 0.9

Table 6. Activity concentrations of the ^{63}Ni in the samples. See Table 4 for description and matrix composition.

ID	^{63}Ni [Bq g^{-1}]	
	EXP.	FLUKA
2	53 ± 6	74.1 ± 22.2
9	81 ± 9	119 ± 45
14	16 ± 3	6.35 ± 6.29
17	80 ± 9	67.1 ± 45.5
31	< 7	NA
32	< 7	NA
33	< 7	NA
36	< 7	NA
38	< 7	NA
39	< 7	NA
40	< 7	NA
42	83 ± 9	23.9 ± 18.5
43	72 ± 8	NA
46	45 ± 6	NA
47	64 ± 7	NA

At the level of p=0.05 there are no statistical differences between the experimental measurements and FLUKA simulations (Tables 4-6). The overall p-value is p=0.86 and it is p=0.42 for ^{54}Mn, p=0.96 for ^{60}Co, p=0.01 for ^{55}Fe and p=0.56 for ^{63}Ni. The case of ^{55}Fe is peculiar: the high uncertainty associated to the experimental determination gives little meaning of the p-value for this radionuclide.

The experimental measures outlined that the presence of gamma and pure beta emitters was far above clearance limits as defined by the "Recommended radiological protection criteria for the recycling of metals from the dismantling of nuclear installations" (RP89) guidelines [24]

Given this good agreement between the experimental results and the simulation, it was decided to use FLUKA to determine the activity per gram for all the main cyclotron components as a function of the time after the last bombardment (Fig. 6); in particular, the activity for each radionuclide after a period of 20 years was calculated (Table 7).

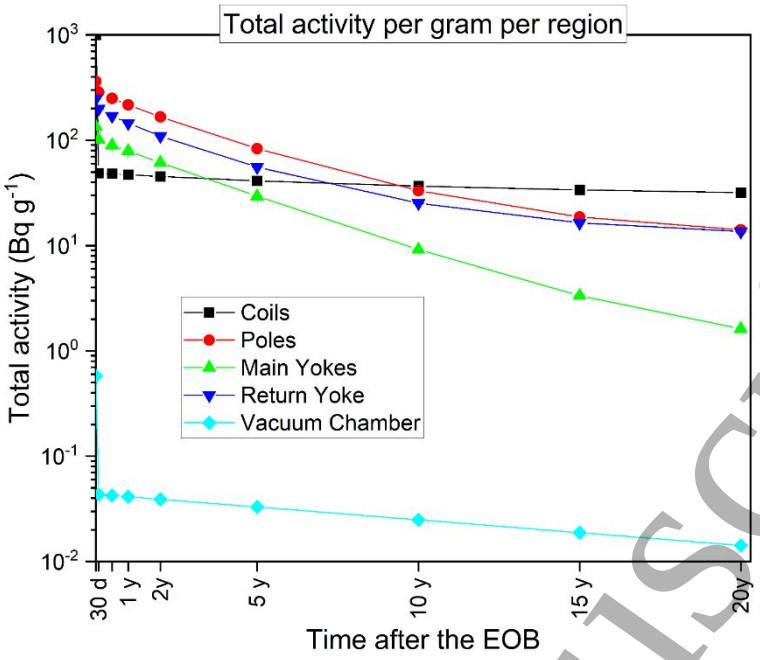

Figure 6. Total activity per gram in function of time after last bombardment.

Table 7. Residual activity for each radionuclide 20 years after the last beam.

Component	Radionuclide	Activity concentration (Bq g^{-1})
Coils	^{60}Co	$3.26 \times 10^{-1} \pm 0.02 \times 10^{-1}$
	^{63}Ni	$3.08 \times 10^{1} \pm 0.01 \times 10^{1}$
Poles	^{60}Co	$2.69 \times 10^{-1} \pm 0.01 \times 10^{-1}$
	^{63}Ni	$6.2 \times 10^{-2} \pm 0.2 \times 10^{-2}$
	^{55}Fe	1.520 ± 0.001
	^{54}Mn	$3.10 \times 10^{-6} \pm 0.01 \times 10^{-6}$
Main Yokes	^{60}Co	$1.182 \times 10^{-1} \pm 0.003 \times 10^{-1}$
	^{63}Ni	$4.4 \times 10^{-3} \pm 0.2 \times 10^{-3}$
	^{55}Fe	$6.242 \times 10^{-1} \pm 0.004 \times 10^{-1}$
	^{54}Mn	$1.70 \times 10^{-7} \pm 0.01 \times 10^{-7}$
Return Yoke	^{60}Co	$1.594 \times 10^{-1} \pm 0.004 \times 10^{-1}$
	^{63}Ni	$6.3 \times 10^{-2} \pm 0.1 \times 10^{-2}$
	^{55}Fe	$9.054 \times 10^{-1} \pm 0.006 \times 10^{-1}$
	^{54}Mn	$4.033 \times 10^{-6} \pm 0.007 \times 10^{-6}$

^{63}Ni, ^{55}Fe and ^{60}Co are the most significant residual nuclides. However, after 20 years (Table 7), the activity concentration of ^{63}Ni and ^{55}Fe is lower than the recycling clearance level [25].

3. CONCLUSIONS

Fifty-three samples from an IBA Cyclone 18/9, a small-scale medical purpose cyclotron were analysed. The residual radioactivity of the nuclides generated in the metal components of the cyclotrons were examined, and the experimental values compared with a FLUKA simulation. In all samples, the principal nuclides detected were ^{63}Ni, ^{54}Mn, ^{60}Co and ^{55}Fe.

The simulation demonstrated that there are no statistical differences as compared to the experimental measurements and suggested that the metal components of the cyclotron should be treated as radioactive waste up to 20 years after shutdown, as the ^{60}Co activity is expected to exceed the recycling clearance level.

The simulation also suggested that the recycling clearance level will be reached after a period ranging from 25 years (for the main yokes) to 30 years (for the magnet coils), once the ^{60}Co activity is lower than 0.1 Bq g^{-1}.

References

[1] Birattari C., Cantone M.C., Ferrari A. and Silari M., "Residual Radioactivity at the Milan AVF Cyclotron", Nucl. Instrum. Methods Phys. Res. B 43, 119-126 (1989).

[2] Eggermont G. "Decommissioning and nuclear waste analysis of a cyclotron". Proceedings of an international conference on nuclear decommissioning. London: ImechE; 1995.

[3] Silari M., "Special radiation protection aspects of medical accelerators", Radiat. Prot. Dosimetry 96(4), 381-92 (2001).

[4] A. Toyoda, G. Yoshida, H. Matsumura, K. Masumoto, T. Nakabayashi, T. Yagishita and H. Sasaki, "Evaluation of induced activity in various components of a PET-cyclotron", J. Phys.: Conf. Ser.1046 012017, 2018

[5] V. Bonvin, F. Bochud, J. Damet, C. Theis, H. Vincke, R. Geyer, "Detailed study of the distribution of activation inside the magnet coils of a compact PET cyclotron", Applied

Radiation and Isotopes, Volume 168, 109446, https://doi.org/10.1016/j.apradiso.2020.109446, 2021

[6] Phillips A., Prull D.E., Ristien R.A. and Kraushaar J.J., "Residual radioactivity in a cyclotron and its surroundings", Health Physics 51, 337-342 (1986).

[7] Kimura K., Ishikawa T., Kinno M., Yamadera A. and Nakamura T., "Residual long-lived radioactivity distribution in the inner concrete wall of a cyclotron vault", Health Physics 67(6), 621-631 (1994).

[8] Sonck M., Buls N., Hermanne A. and Eggermon G., "Radiological and Economic Impact of Decommissioning Charged Particle Accelerators", IRPA 10 25, 207-226 (2000).

[9] L.R.Carroll, "Predicting long-lived, neutron-induced activation of concrete in a cyclotron vault", AIP Conference proceedings, vol.575(1), 301-304 (2001)

[10] S. Vichi, A. Infantino, F. Zagni, G. Cicoria, S. Braccini, D. Mostacci, M. Marengo, "Activation studies for the decommissioning of PET cyclotron bunkers by means of Monte Carlo simulations", Radiation Physics and Chemistry, Volume 174, 108966, https://doi.org/10.1016/j.radphyschem.2020.108966, 2020.

[11] Urabe I. et al., "Depth distribution of residual radioactivity in the concrete wall of an electron linac facility", Health Physics 60, 587- 591 (1991).

[12] Hermanne A et al., "Decommissioning medical linear accelerators: a study on identification and minimization of nuclear waste", Symposium of the Belgian Hospital Physicists Association, Antwerp (1999).

[13] J. Blaha, F.P. La Torre, M. Silari, J. Vollaire, "Long-term residual radioactivity in an intermediate-energy proton linac", Nuclear Instruments and Methods in Physics Research Section A: Accelerators, Spectrometers, Detectors and Associated Equipment, Volume 753, Pages 61-71, https://doi.org/10.1016/j.nima.2014.03.058, 2014.

[14] Cristian Bungau, Adriana Bungau, Robert Cywinski, Roger Barlow, Thomas Robert Edgecock, Patrick Carlsson, Håkan Danared, Ferenc Mezei, Anne Ivalu Sander Holm, Søren

Pape Møller, and Heine Dølrath “Thomsen, Induced activation in accelerator components”, Phys. Rev. ST Accel. Beams 17, 084701 – Published 18 August 2014

[15] Calandrino R, del Vecchio A, Savi A, Todde S, Griffoni V, Brambilla S, Parisi R, Simone G, Fazio F. “Decommissioning procedures for an 11 MeV self-shielded medical cyclotron after 16 years of working time”. Health Phys. 2006 Jun;90(6):588-96. doi: 10.1097/01.HP.0000190161.96172.ae

[16] Hermanne, Alex; Sonck, Michel. “Evaluation of the radiological and Economic Consequences of Decommissioning Particle accelerators”. EUR 19151 EN European Commission, Nuclear Safety and the Environment, 1999.

[17] A. Ferrari, P.R. Sala, A. Fasso`, and J. Ranft, "FLUKA: a multi-particle transport code" CERN-2005-10 (2005), INFN/TC_05/11, SLAC-R-773

[18] T.T. Böhlen, F. Cerutti, M.P.W. Chin, A. Fassò, A. Ferrari, P.G. Ortega, A. Mairani, P.R. Sala, G. Smirnov and V. Vlachoudis, "The FLUKA Code: Developments and Challenges for High Energy and Medical Applications", Nuclear Data Sheets 120, 211-214 (2014)

[19] V.Vlachoudis "FLAIR: A Powerful But User Friendly Graphical Interface For FLUKA" Proc. Int. Conf. on Mathematics, Computational Methods & Reactor Physics (M&C 2009), Saratoga Springs, New York, 2009

[20] Currie LA, “Limits for qualitative detection and quantitative determination. Application to radiochemistry” Anal Chem 40:586, 1968

[21] ISO 11929-1, “Determination of the characteristic limits (decision threshold, detection limit and limits of the coverage interval) for measurements of ionizing radiation -- Fundamentals and application Elementary applications”, 2019

[22] IAEA – INTERNATIONAL ATOMIC ENERGY AGENCY, Decommissioning of Medical, Industrial and Research Facilities, IAEA Safety Standards Series No. SSG-49, IAEA, Vienna (2019).

[23] Calandrino R, del Vecchio A, Savi A, Todde S, Belloli S. “Intake risk and dose evaluation methods for workers in radiochemistry labs of a medical cyclotron facility”. Health Phys. 2009 Oct;97(4):315-21. doi: 10.1097/HP.0b013e3181ad8192.

[24] European Commision, “Recommended radiological protection criteria for the recycling of metals from the dismantling of nuclear installations – RP89”, 1998

[25] IAEA – INTERNATIONAL ATOMIC ENERGY AGENCY, Clearance Levels for Radionuclides in Solid Materials: Application of Exemption Principles Interim Report for Comment, IAEA-TECDOC-855, IAEA, Vienna (1996).